Measurement of $\mathrm{G_E^n/G_M^n}$ by the Double Polarised ${}^2\mathrm{H}(\overrightarrow{e}, e'\overrightarrow{n})$ Reaction

How high in Q^2 can be attained?

John R.M. Annand
School of Physics and Astronomy
University of Glasgow

Electromagnetic Form Factors (EMFF) in JLab Hall A

All 4 Nucleon Sachs form factors.

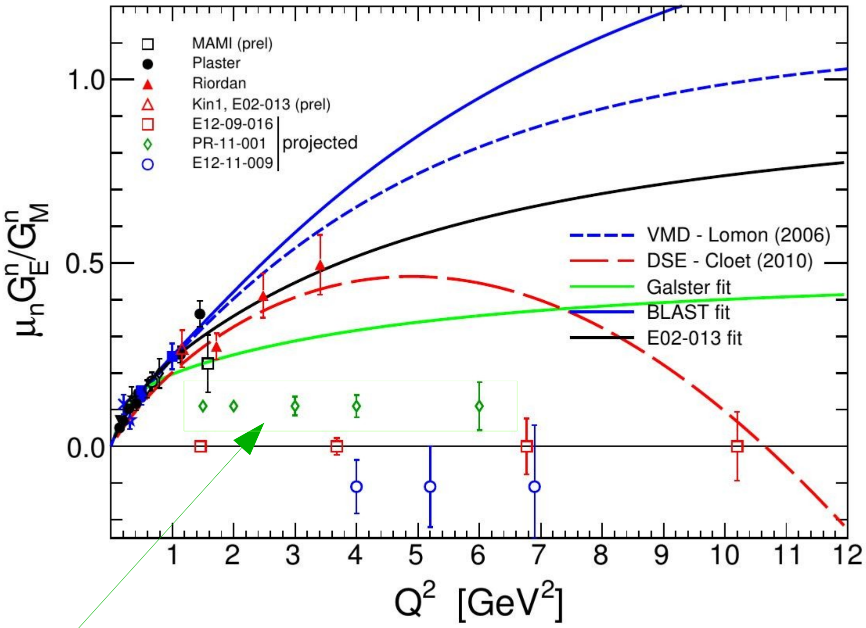

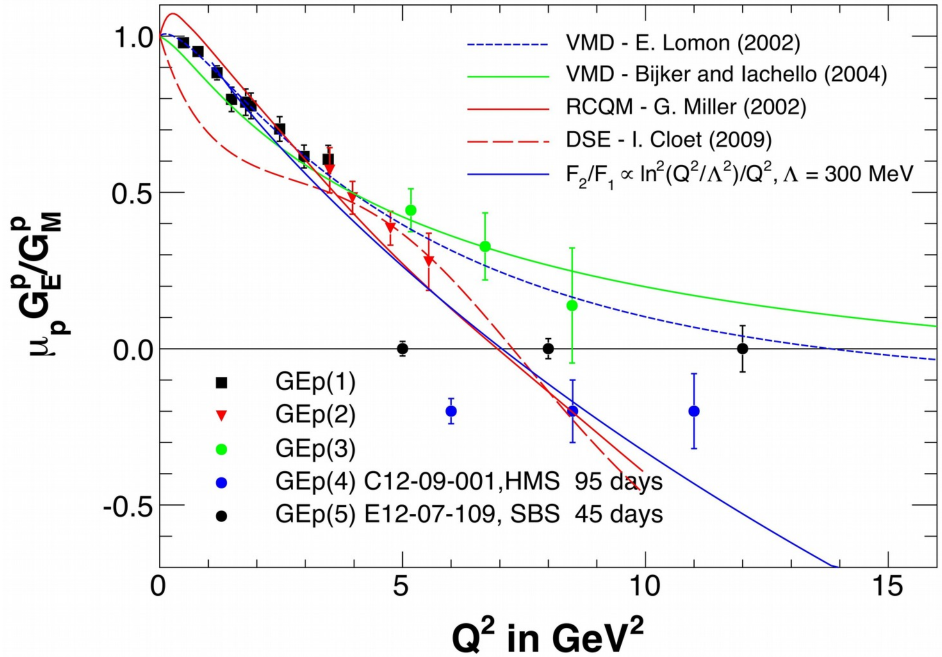

G_{En}/G_{Mn} PR12-11-001

Cross Section

$$\sigma_{ep} \propto \frac{E^2}{Q^{12}}$$

Polarimetry

$$A_y \propto \frac{1}{p_p} \sim \frac{M}{Q^2}$$

$$FOM \propto NA_y^2 \sim \frac{E^2}{Q^{16}}$$

HRS allows absolute measurement to 1 – 2% accuracy
E12-07-108 G_{Mp} elastic *H(e,e'p)*

SBS programme of nucleon EMFF measurements

- E12-09-019 G_{Mn}/G_{Mp} (by ratio *d(e,e'n)/d(e,e'p)* method)
- E12-09-016 G_{En}/G_{Mn} (with polarized beam & target)
- E12-07-109 G_{Ep}/G_{Mp} (with polarized beam & recoil polarimetry)

Zero Crossing Point of G_E/G_M

J. Segovia et al., Few-Body Syst. 55 (2014), 1185.
DSE common framework N-elastic and Δ-transition form factors

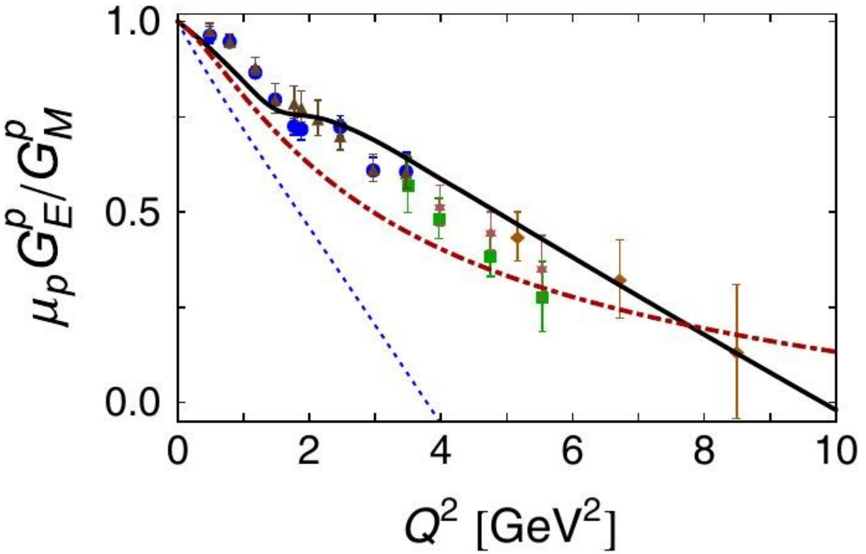

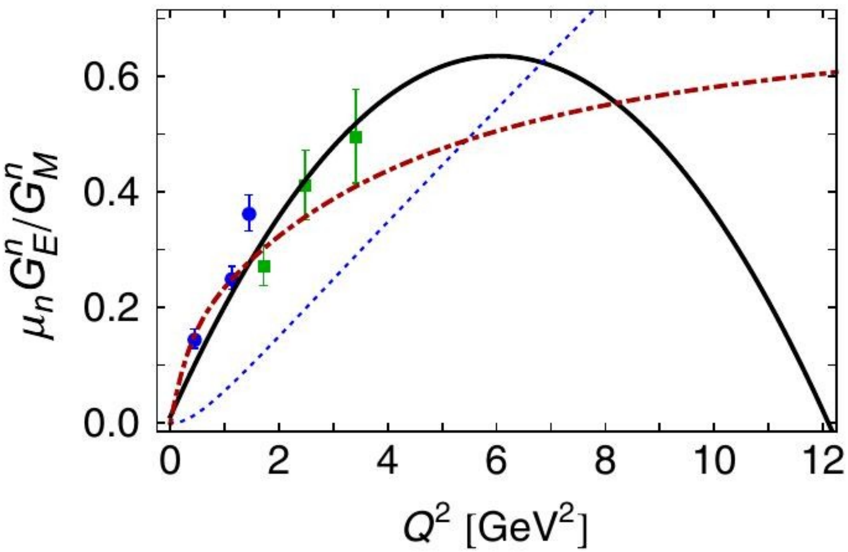

- DSE explicitly describe the dynamical generation of the mass of constituent quarks
- Zero crossing point (if any) of the G_E/G_M ratios affects the location and width of the transition region between constituent- and parton-like behavior of the dressed quarks.
- A more rapid transition from non-perturbative to perturbative behavior pushes the proton zero point to higher Q^2
- Conversely the neutron zero point is pushed to lower Q^2
- Neutron data completely lacking at high Q^2

EMFF and Diquark Correlations in Nucleons

Calculation: *I.Cloet et al., Phys. Rev. C 90, 045202 (2014)*

Dirac FF

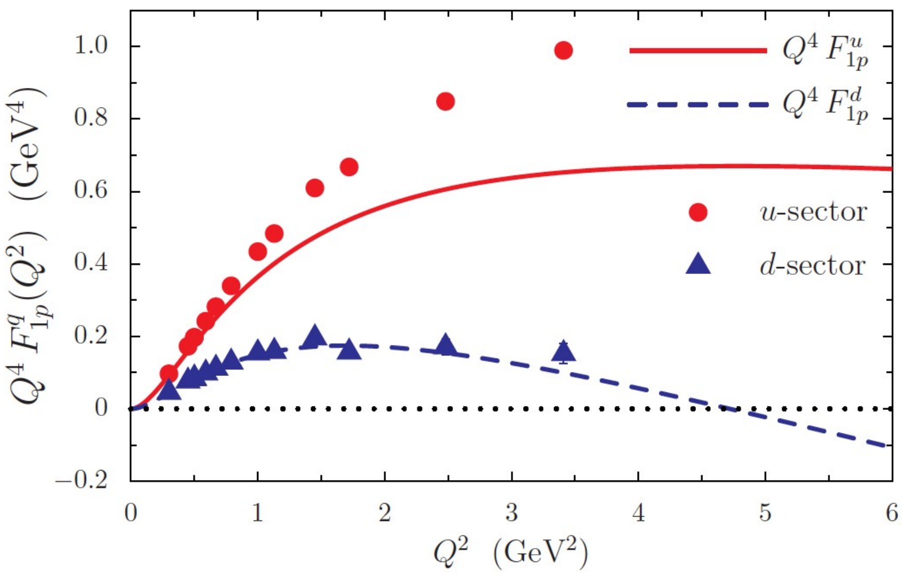

Pauli FF

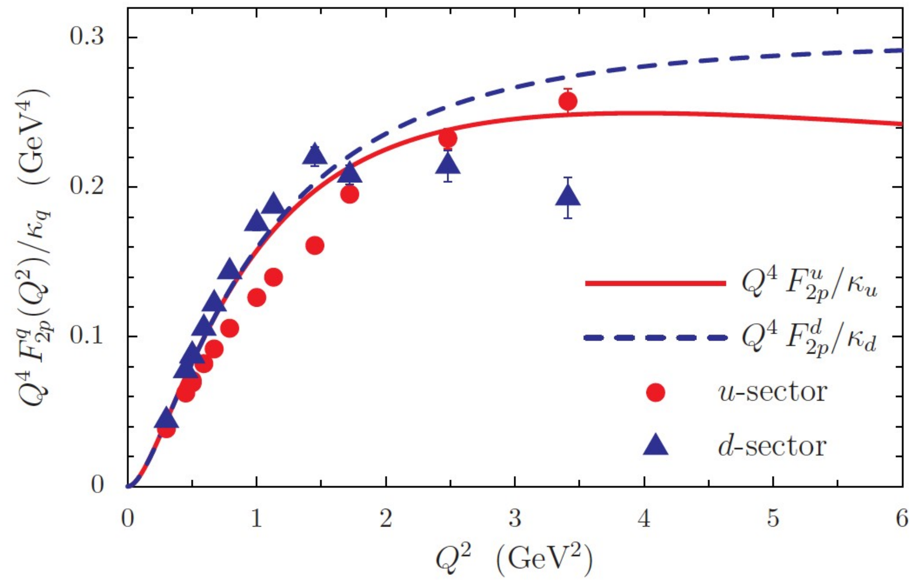

Separated data points: *G. D. Cates et al., Phys. Rev. Lett. 106, 252003 (2011).*

With **Proton & Neutron EMFF data** flavour decomposition possible
Assuming small strange component: $F^u_{1,2} = F^n_{1,2} + 2F^p_{1,2} \quad F^d_{1,2} = 2F^n_{1,2} + F^p_{1,2}$

- Calculation using Nambu-Jona-Lassinio Model
  Chiral Effective Field Theory of QCD
  Valid @ low-intermediate energy
  "Parameter free" calculation. No. FF fit.
- "Soft" d Dirac FF: dominance of scalar diquark correlations
- Pauli FF: axial-vector diquark correlations and pion-cloud effects more important
- Q^2 range of decomposition set by availability of G_{En} data

The Need for Better G_{En}/G_{Mn} Data

- In terms of Q^2 range and precision, neutron measurements still lag way behind proton measurements
- For measurements in space-like domain at medium-high Q^2 JLab is the only viable lab. Quasi-elastic electron scattering from neutron in ^{2}H, ^{3}He...
- Double polarised experiments are the way to go (since ~ 1990)
  Relatively low sensitivity to two-photon exchange effects compared to Rosenbluth separation
  Better access to relatively small G_E (compared to G_M)
- JLab: E12-09-016 G_{En}/G_{Mn} with polarized electron beam & ^{3}He target up to Q^2 of ~10 $(GeV/c)^2$...see talk by S. Riordan
- Neutron measurements extremely challenging...independent verification of results necessary
  Alternative method with polarised electron beam and polarimeter to measure polarisation transfer to recoiling neutron. Unpolarised ^{2}H target
- QE signal much cleaner with ^{2}H target compared to ^{3}He
- ^{2}H experiment should, as far as possible, match kinematic range and precision of ^{3}He experiment.
- Up to now no recoil polarimetry measurement at $Q^2 > 1.5$ $(GeV/c)^2$

Summary of Experimental Method

Obtain G_{En}/G_{Mn} for Q^2 of 2.0 – 9.3 ? $(GeV/c)^2$

Measure double-polarised $^2H(\overrightarrow{e}, e'\overrightarrow{n})p$

As opposed to E12-09-016 $\overrightarrow{^3He}(\overrightarrow{e}, e'n)pp$

- Final-state neutron P_x/P_z → G_{En}/G_{Mn} (precess P_z → P_y in dipole magnetic field)
- Cryogenic D_2 Target 10 cm long
- 40 µA 80% polarized electron beam
- $L = 1.26 \times 10^{38}\ cm^{-2}s^{-1}$
- BigBite e' detector (same configuration as E12-09-019 G_{mn}/G_{mp})

  Large acceptance (~ 55 msr), adequate momentum resolution (δp/p ~ 1%)
- SBS Neutron polarimeter: acceptance well matched to electron arm
  Dipole magnet, integrated field ~ 2 Tm
  Hadron calorimeter, high n efficiency, effective suppression soft background
  Active organic-material analyzer
  High rate charged-particle tracking systems
- Still examining polarimeter configurations...active/passive analyser?
  Geant-4 simulation

G_{En}/G_{Mn} Methods...Pros & Cons

Polarized Target Neutron or Polarized Recoiling Neutron?

Advantages Recoil Polarimetry

- ^{3}He target is complex and expensive
- ^{2}H (liquid) target offers higher luminosity (if detectors will stand the radiation load)
- Quasi-elastic scattering on ^{2}H gives a cleaner signal than ^{3}He...less non-elastic contamination
- Bound-nucleon effects smaller for ^{2}H

Disadvantages Recoil Polarimetry

- For n-p analysing power A_y prop. $1/p_N$
  Experiment FOM prop. A_y^2 (or P^2_{target})
  $A_y \sim 0.05$, $P_{target} \sim 0.6$
- Nucleon polarimeter has relatively low detection efficiency (n scattering)
- Up to now no recoil-polarimetry measurement beyond $Q^2 = 1.5\ (GeV/c)^2$ Hall-C
  Plaster et al, PRC 73,(2006), 025205

Peak Analysing Power of N-N Scattering
A_y^{max} @ $p_\perp \sim 300$ - 400 MeV/c

●■ R. Diebold et al., PR. 35(1975), 632.
S.L. Kramer et al., PRD17(1978), 1709.
Projection n-p momentum dependence E12-11-009
Projection n-p momentum dependence PR12-12-12

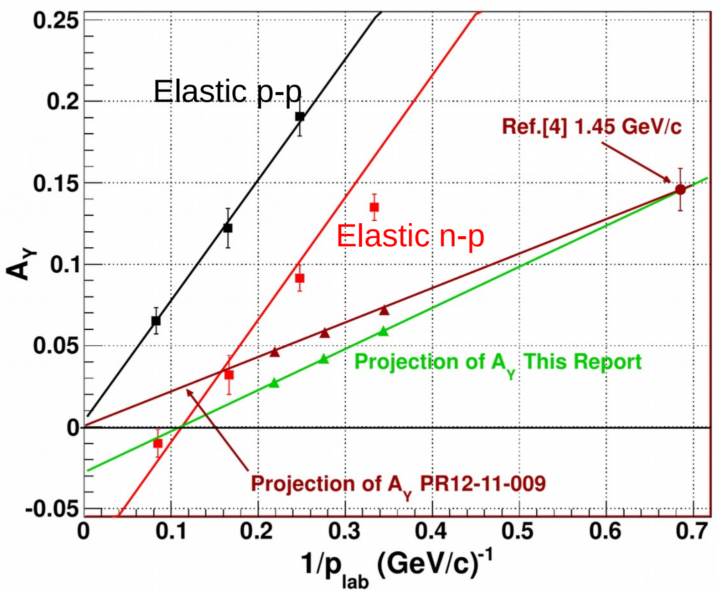

- Hydrogen in principle the best analyser
- C, CH_2 used in practice
- For neutrons can use plastic scintillator or Cherenkov ?...active analyzer highly desirable to reconstruct scattering kinematics

G_E/G_M using Recoil Polarimetry

R.G.Arnold, C.E.Carlson and F.Gross, Phys.Rev. C23(1981),363
A.I.Akhiezer et al., JEPT 33 (1957),765

$$
\begin{aligned}
P_x &= -hP_e \frac{2\sqrt{\tau(1+\tau)}\tan\frac{\theta_e}{2} G_E G_M}{G_E^2 + \tau G_M^2 (1+2(1+\tau)\tan^2\frac{\theta_e}{2}} \\
P_y &= 0 \\
P_z &= hP_e \frac{2\tau\sqrt{1+\tau+(1+\tau)^2\tan^2\frac{\theta_e}{2}}\tan\frac{\theta_e}{2} G_M^2}{G_E^2 + \tau G_M^2 (1+2(1+\tau)\tan^2\frac{\theta_e}{2})} \\
\frac{P_x}{P_z} &= \frac{1}{\sqrt{\tau+\tau(1+\tau)\tan^2\frac{\theta_e}{2}}} \cdot \frac{G_E}{G_M}
\end{aligned}
$$

Recoil Polarimetry...
N-N scattering $V_{so}(\boldsymbol{l.s}) \rightarrow$
ϕ dependence of cross section relates to transverse polarisation components

$$\sigma(\theta'_n, \phi'_n) = \sigma_\circ \left(1 + P_e \alpha_{eff} \left[P_x^n \sin\phi'_n + P_y^n \cos\phi'_n\right]\right)$$

Precession angle of nucleon P_z through dipole

$$\chi = \frac{2\mu_N}{\hbar c \beta_N} \int_L B.dl$$

Integrated Field ~2 Tm: $\chi \rightarrow 70°$ as $\beta_n \rightarrow 1$

Scattering asymmetry blocks detect neutrons or protons...
Here: Fe/Plastic segmented calorimeter HCAL

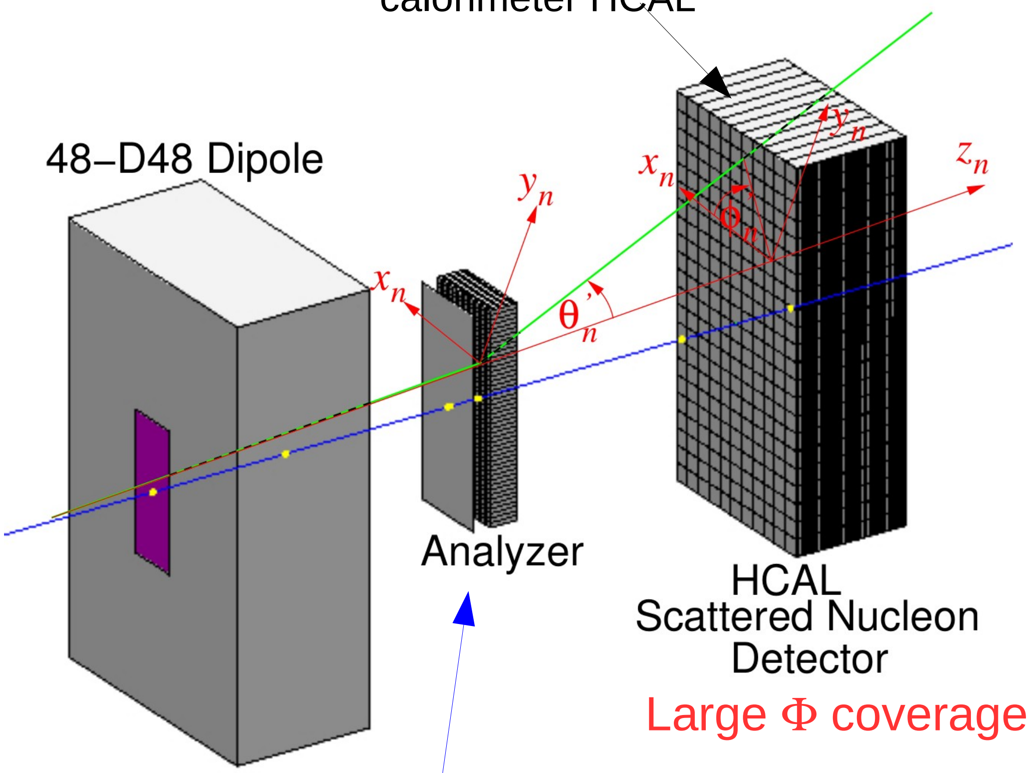

Large Φ coverage

Analyser block for neutrons active (e.g. plastic scintillator) and position sensitive. Use both elastic n-p and quasi-elastic n-p from ^{12}C

Elastic N-N Scattering

- Elastic n-p or p-p for highest A_y value. LH_2 analyser possibly not feasible technically at JLab
- Proton A_y measurements C, CH_2: detect forward proton + X undetected
  This does not select elastic or quasi-elastic exclusively
- Empirical p+C value of A_y ~0.5 of free elastic p-p scattering
  Partially fermi-motion smearing of the elastic signal
  Partially inelastic contamination
- Advantageous to detect forward scattered nucleon
  Smaller spread in angles
  High energy...threshold can be set to reject low-energy background

Peak Analysing Power of N-N Scattering
A_y^{max} @ $p_\perp$ ~ 300 - 400 MeV/c

R. Diebold et al., PR. 35(1975), 632.
S.L. Kramer et al., PRD17(1978), 1709.
L.S. Azhgirey et al., NIM A538(2005), 431.
N.E. Cheung et al., NIM A363(1995), 561.
I.G. Alekseev et al., NIM A434(1999), 254.

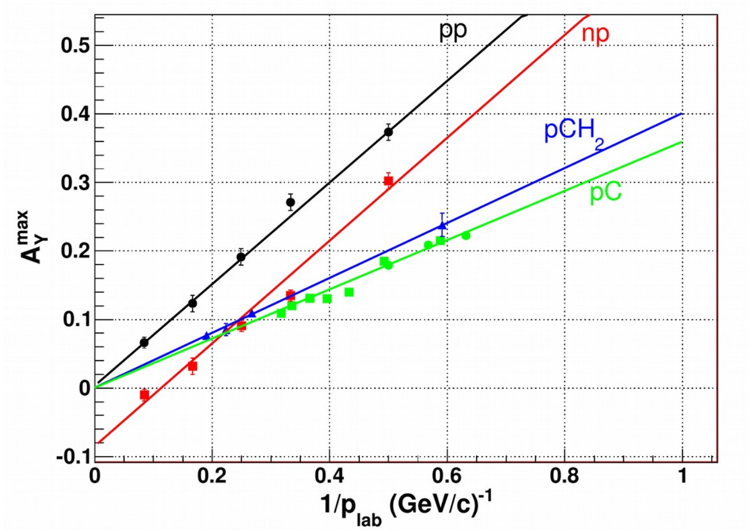

Angular spread in quasi-elastic
$n + {}^{12}C \rightarrow n + p + {}^{11}B$
Quasi-elastic on bound neutron would not give signal in active analyser

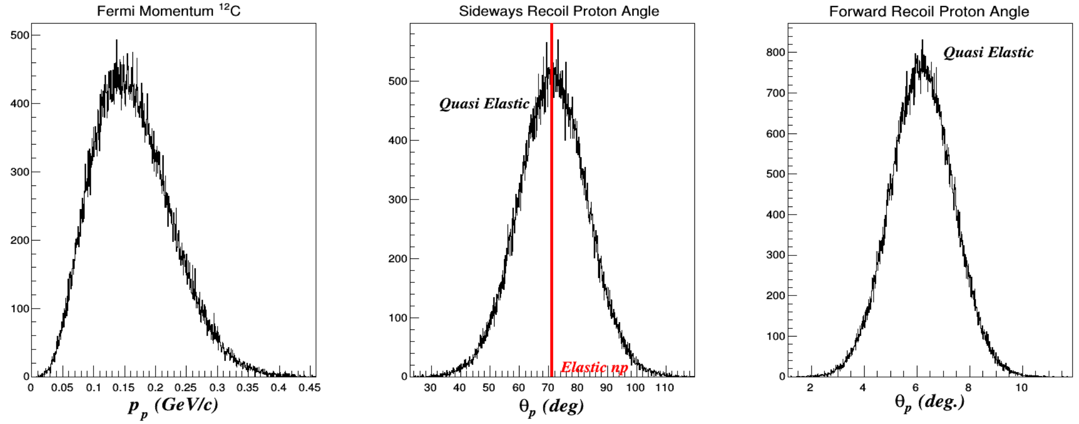

n-p Elastic: Forward Neutron vs. Forward Proton

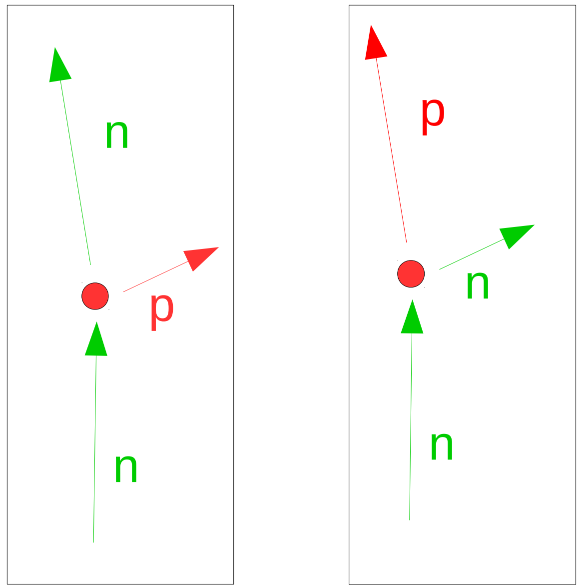

Diebold et al., PRL 35,(1975),632
Fits: Ladygin JINR E13-99-123 (1999)

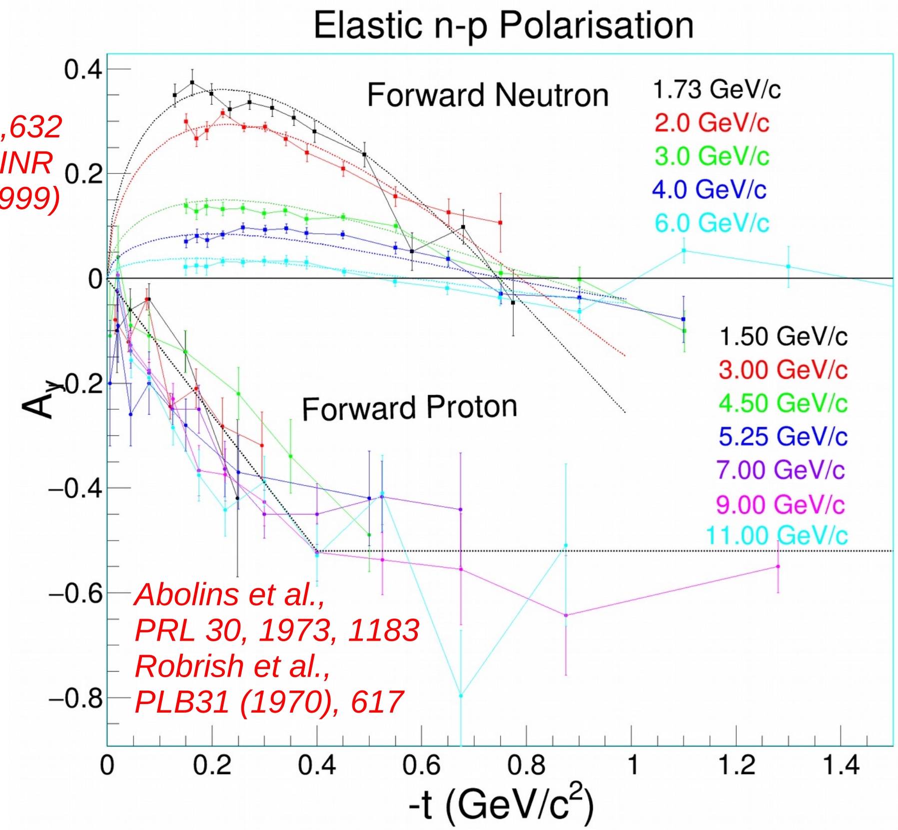

- Measurements from 1970's
- A_y for n-p (or p-n) falling rapidly with increasing neutron momentum
- A_y for charge-exchange n-p large at sufficiently large t (θ_p ~ few deg.)
  No apparent strong incident momentum dependence of A_y
- Charge-exchange cross section factor ~10 lower than n-p
  SAID PWA over estimates this cross section by a factor ~6

SAID PW analysis & data base
https://ins.columbian.gwu.edu/data-analysis-center

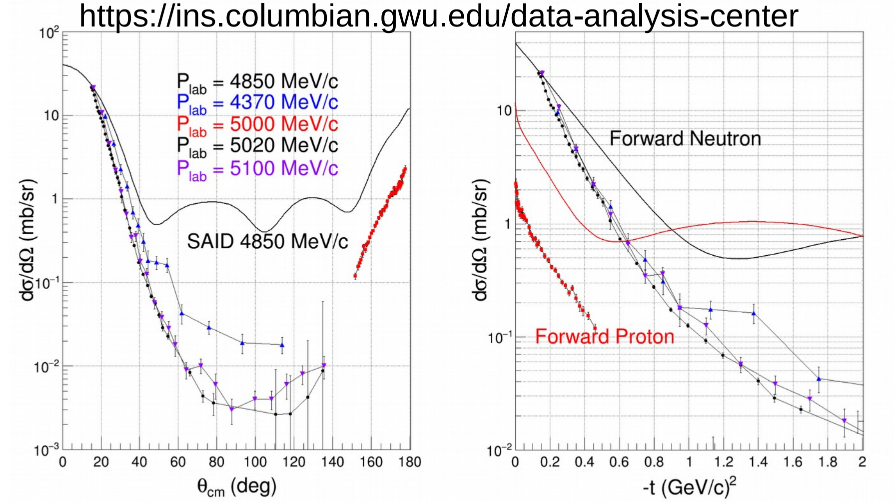

Preliminary: Polarimeter Figure of Merit

Neutron Scattering in Analyzer Material

$$\sigma(\theta_n^{'}, \phi_n^{'}) = \sigma(\theta_n^{'}) \left[1 + A_y(\theta_n^{'}) \left\{ P_x^n \sin\phi_n^{'} + P_y^n \cos\phi_n^{'} \right\}\right]$$

Monte Carlo: ROOT & G4

- Generate elastic n(e,e'n)
  produce n-momentum distribution
  n scatters from analyzer block
  into HCAL
- n-p cross section SAID PWA.
  × [1 + (effective# protons in C)]
  Scale charge-exchange by 0.16
  Efficiency ~ 7-8%
- Efficiency from G4 ~ 12-13%
- A_y for n-p scatter (forward n)
  Ladygin (JINR) fit to p_n and t dependence
- A_y charge-exch. n-p (forward p)
  $A_Y^H = t, -t < 0.4;\ A_Y^H = -0.52, -t > 0.4$
  $A_Y^C = 0.5 \times A_Y^H$
- SBS polarimeter sensitive to both n-p and charge-exchange n-p

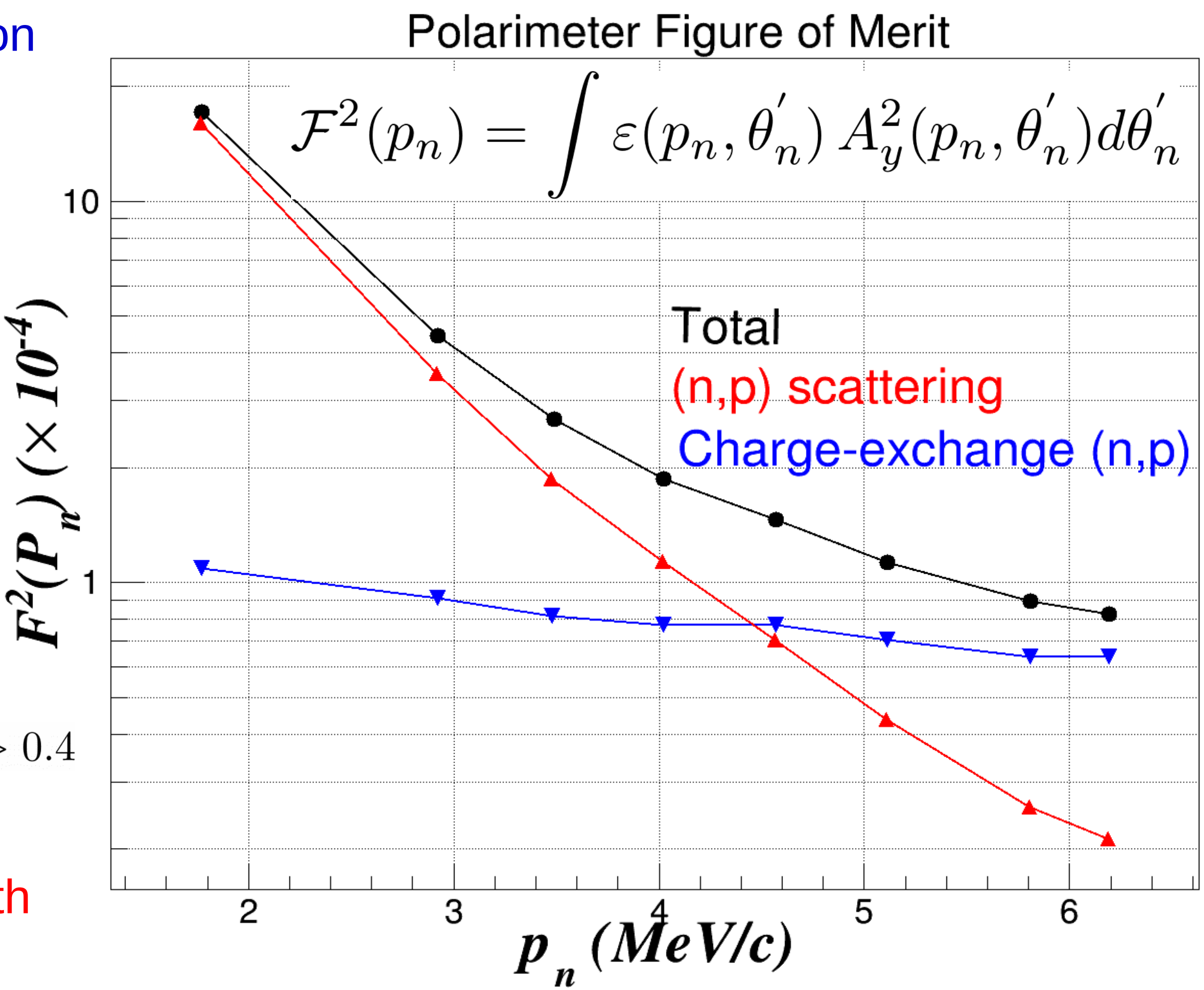

G_{En} Apparatus $e + d \rightarrow e' + n + p$

Explore possibility to use G_{Ep} polarimeter charge-exchange n-p

10cm LD_2 Target

40 µA beam 4.4 - 8.8 GeV

$\mathfrak{L}$: 1.26×10^{38} cm^{-2} s^{-1} per nucleon

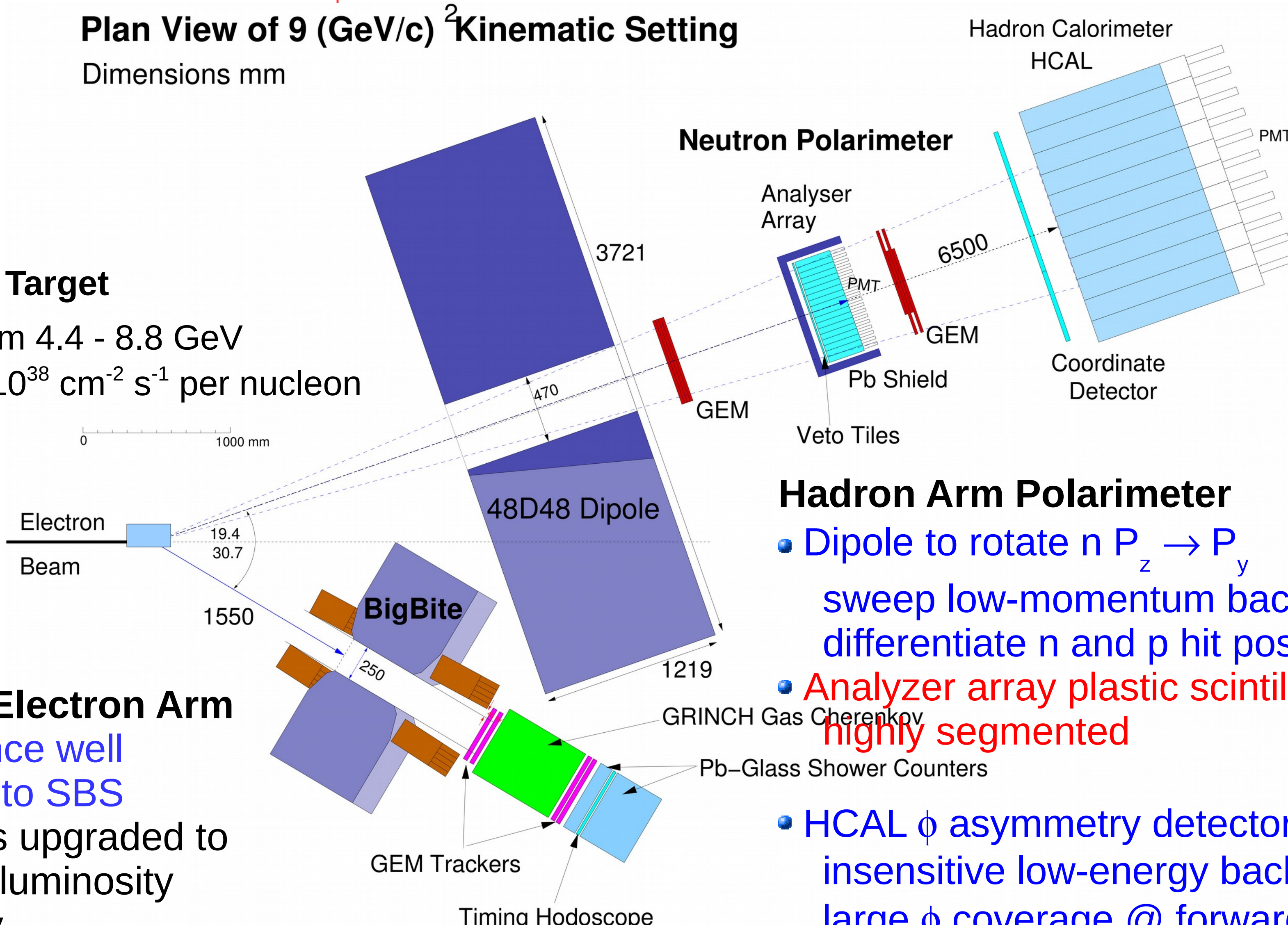

Hadron Arm Polarimeter

- Dipole to rotate n $P_z \rightarrow P_y$
  sweep low-momentum background
  differentiate n and p hit positions
- Analyzer array plastic scintillator
  highly segmented
- HCAL ϕ asymmetry detector
  insensitive low-energy background
  large ϕ coverage @ forward θ

BigBite Electron Arm

Acceptance well matched to SBS

Detectors upgraded to increase luminosity capability

The Geant-4 Model

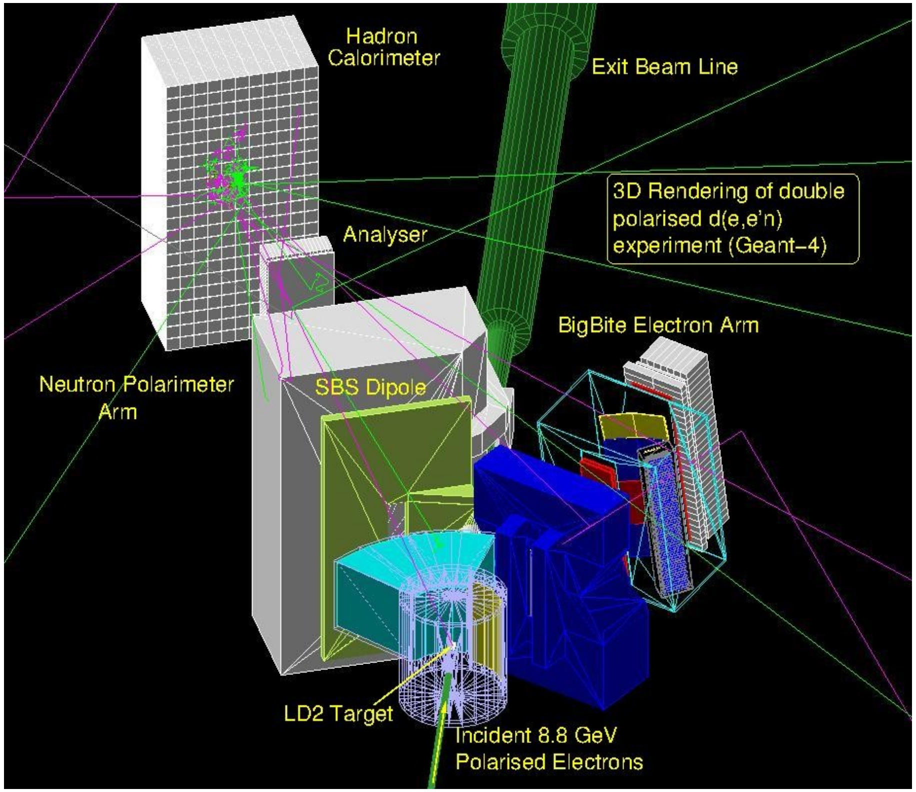

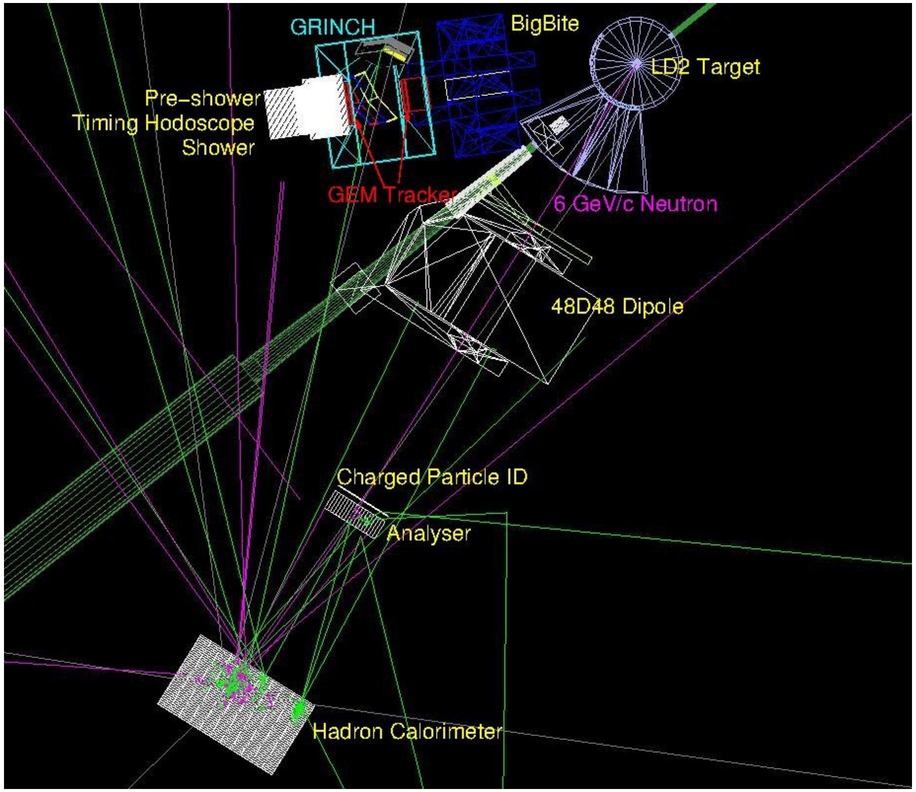

- Geant4.10.01: add ϕ dependence polarised nucleon elastic and QE scattering
- Record signal amplitude and time from each detector element.
- Analyse simulated data as in real experiment.
- Calculate element rates 8.8 GeV, 40 μA on 10 cm LD_2 ($\mathfrak{L} = 1.26 \times 10^{38}$ $cm^{-2}s^{-1}$)
- Concentrating on polarimeter arm. Cluster analysis, energy-weighted mean hit position
- Reconstruct angle in analyser and scattering angle analyser to calorimeter. Extract ϕ dependence.

Detector Rates: Analyser Array

Analyser: Individual Element Singles Rates

GEANT-4

DINREG

Ebeam (GeV)	Angle (deg)	Shield	Element	Threshold (MeV)	Rate (kHz)
8.8	19.4	No Pb	Single Bar	1.0	14000
8.8	19.4	No Pb	Single Bar	5.0	2800
8.8	19.4	50mm Pb	Single Bar	1.0	1800
8.8	19.4	50mm Pb	Single Bar	5.0	230
8.8	19.4	50mm Pb	Hit Cluster	20.0	71
4.4	27.5	50mm Pb	Single Bar	1.0	830
4.4	27.5	50mm Pb	Single Bar	5.0	95
4.4	27.5	50mm Pb	Hit Cluster	20.0	14
4.4	27.5	50mm Pb	Single Bar	1.0	1000
4.4	27.5	50mm Pb	Single Bar	5.0	200

Geant4.10.01 calculated rates consistent with previous DINREG calc. (Geant-3)

- Most demanding kinematics
  $Q^2 = 9.3\ (\mathrm{GeV}/c)^2$, $L = 1.26 \times 10^{38}$
  Beam energy 8.8 GeV
  BigBite @ 30.7 deg.
  Polarimeter @ 19.4 deg.
- Pb shield necessary when using plastic scintillator for analyser
- Analyser option: use plexi-glass Cherenkov? ...doesn't help much if most of background soft photons
  Polyethylene CH_2...optically OK?

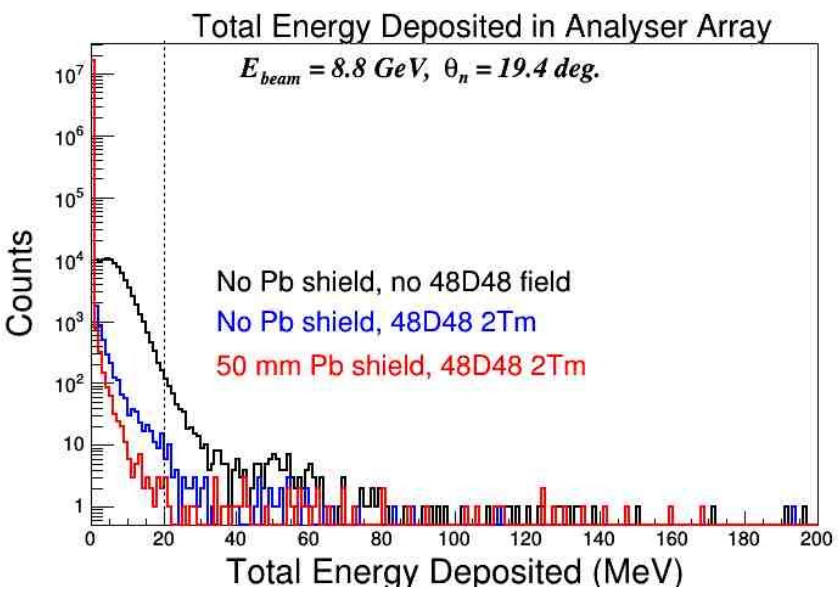

6 GeV/c neutrons incident on Analyser

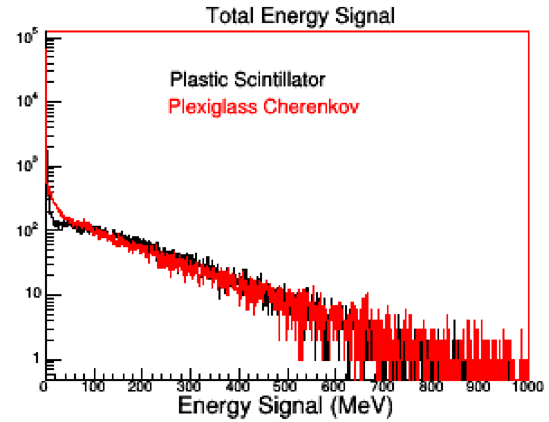

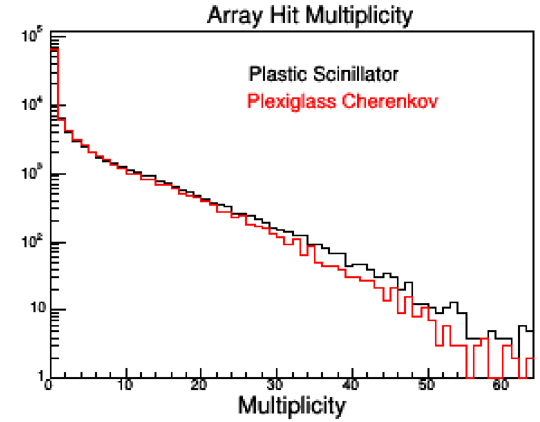

Normalise Scintillator/Cherenkov signals to proton energy loss

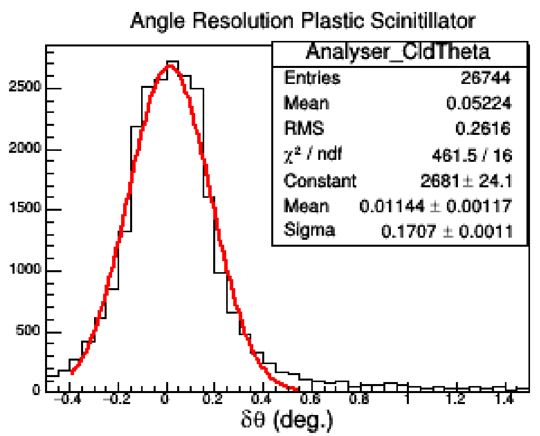

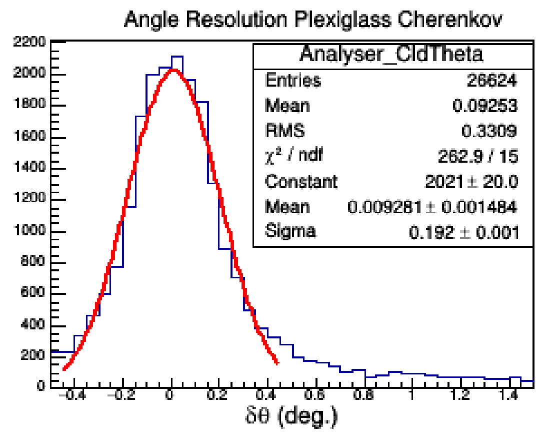

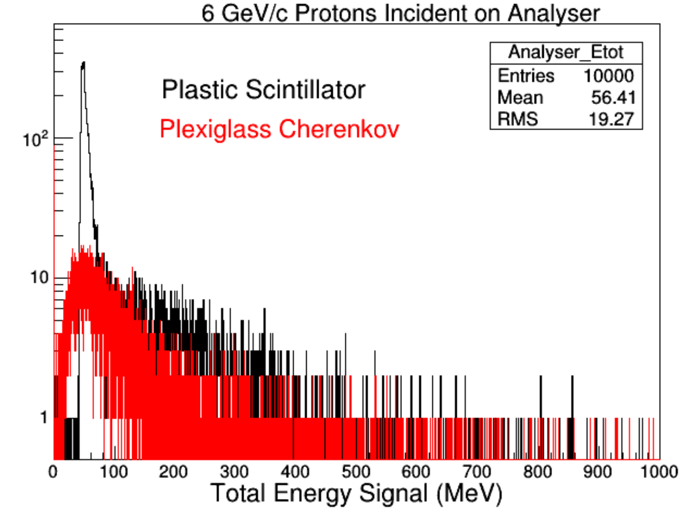

- 18x46 array of 4 x 4 x 25 cm plastic scintillator aligned parallel direction incident neutrons
- Energy weighted cluster analysis: apply cluster energy threshold 20 MeV, angle resolution 0.17 deg.
- Plastic scintillator detection efficiency 26% for 6 GeV/c incident neutrons
- Calculation for plastic scintillator and plexiglass Cherenkov. Slightly lower efficiency for plexiglass

Calorimeter

- 11 x 22 array of 15 x 15 x 90.8 cm modules
- Each module
  40 sheets 1 cm thick plastic scint.
  40 sheets 1.27 cm thick Fe
  Central WLS readout strip
- Trigger on events of “total-energy” > ½ peak channel value of cluster energy
- Position resolution ~ 4 cm @ 6 GeV/c from energy weighted cluster analysis
- Detection efficiency 6 GeV/c neutrons 77%
- Forward angle protons: can use CDet and GEM for better track determination

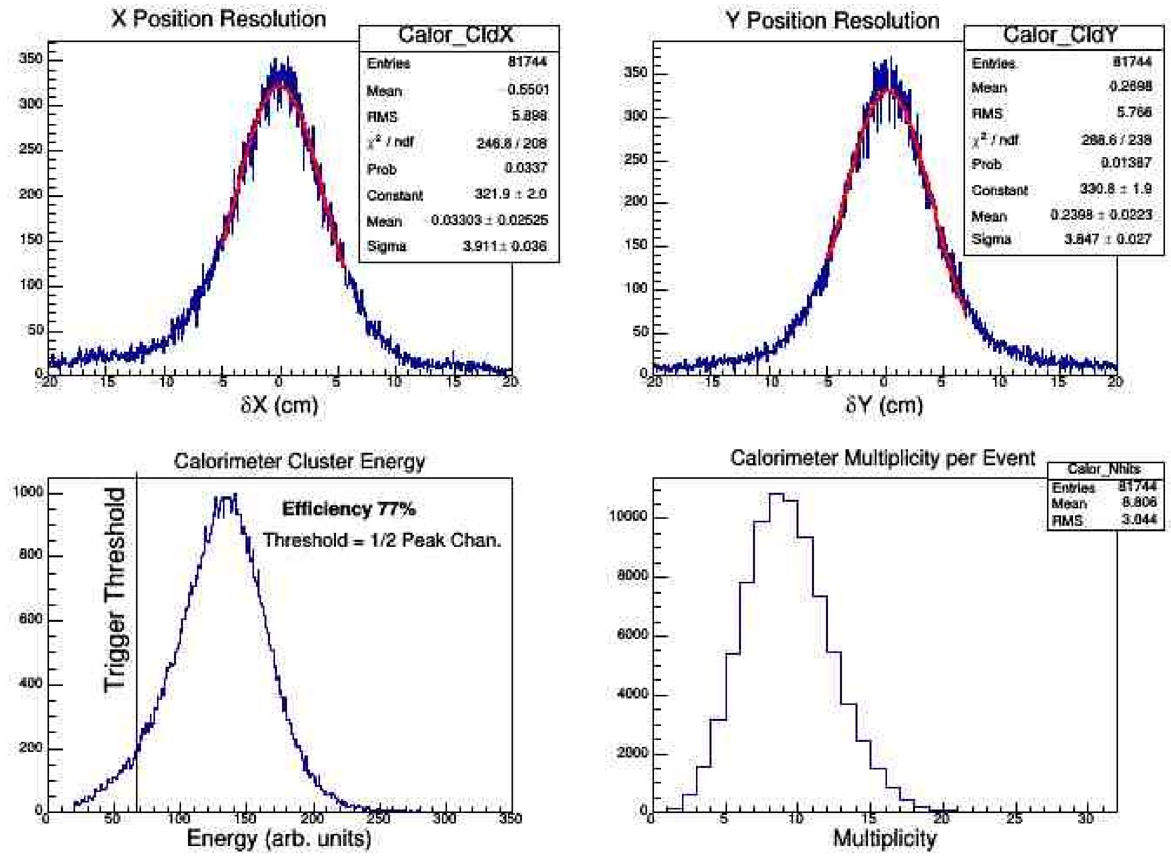

Polarimeter

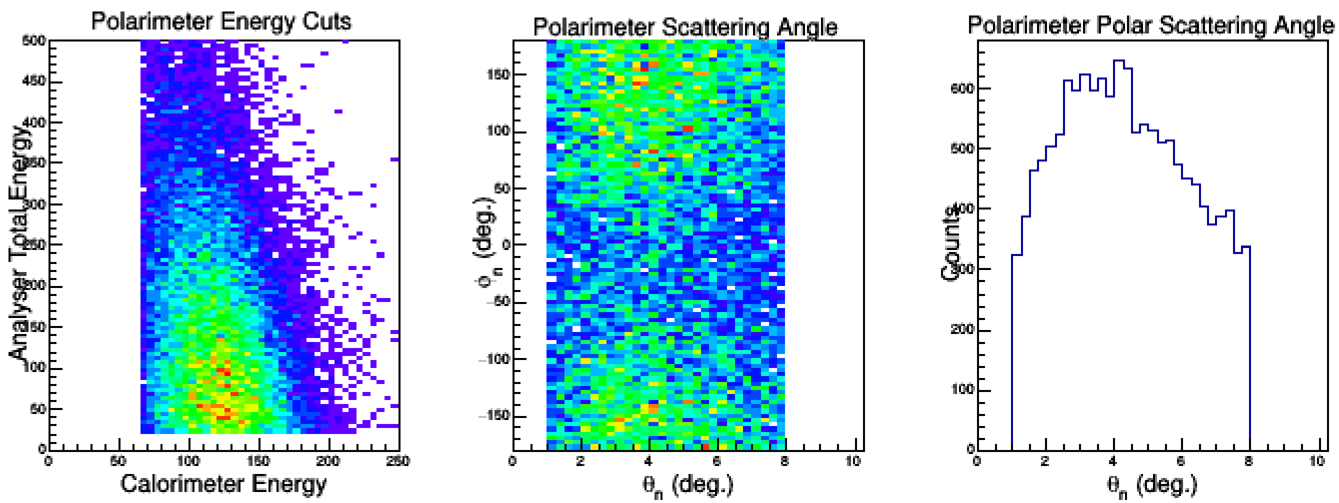

- Optimum scattering angle depends on incident neutron momentum
  Distance from analyser to calorimeter adjustable
- 6 GeV/c incident neutrons
  Select analyser energy deposit > 20 MeV
  Select calorimeter energy deposit > ½ peak channel
  Select polar scattering angle θ_n 1 – 8 deg.
- Polarimeter detection efficiency 13.9% (not all of that is from elastic or quasi-elastic scattering)

Obtaining Polarisation Components $P_x P_y$

$$\sigma(\theta_n, \phi_n) = \sigma(\theta_n)\left\{1 + P_e A_y^{eff}(P_x \sin\phi_n + P_y \cos\phi_n)\right\}$$

- 4 Comb. beam helicity, SBS dipole polarity

$$F(\phi_n) = C\{1 \pm |P_x^*| \sin\phi_n \pm |P_y^*| \cos\phi_n\}$$

- **Unpolarized Distribution**

$$C = (F_{++} + F_{--} + F_{+-} + F_{-+})/4$$

- **Polarized Distributions**

$$F_x = (F_{++} - F_{-+} + F_{+-} - F_{--})/2C$$
$$F_y = (F_{++} - F_{+-} + F_{-+} - F_{--})/2C$$

- **4×10^5 incident neutrons, 6 GeV/c**
  Input polarisation components
  Incl. $P_e = 0.8$; $\chi(z \rightarrow y) = 70^o$
  $P_x = 0.190$, $P_y = 0.524$, $A_y = 1.0$
- Reconstructed polarisation comp.

$$P_x^* = 0.109 \pm 0.009; \quad A_y^{eff} = 0.574 \pm 0.045$$
$$P_y^* = 0.316 \pm 0.009; \quad A_y^{eff} = 0.603 \pm 0.017$$

$$\mathcal{F}^2 \sim \epsilon(A_y^{eff})^2 = 0.14 \times 0.59^2$$

$$\delta P = \sqrt{\frac{2}{4 \times 10^5 \times \mathcal{F}^2}} = 0.01$$

Simulated Data

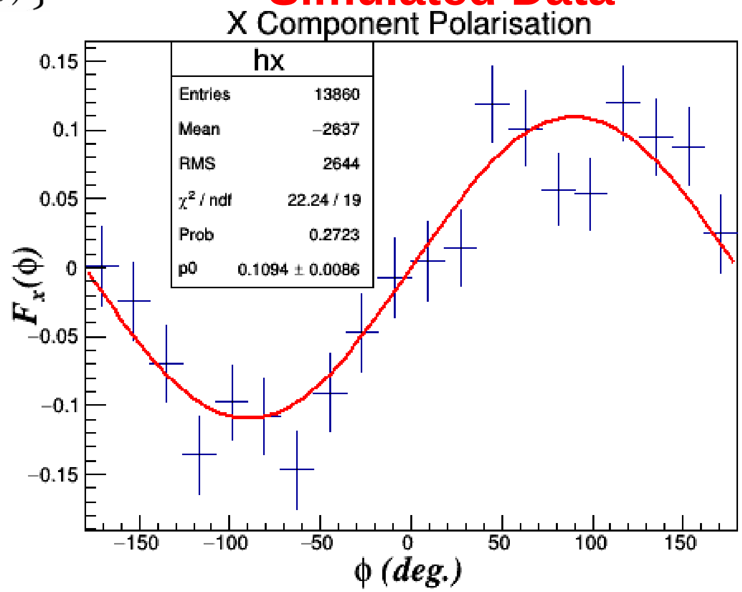

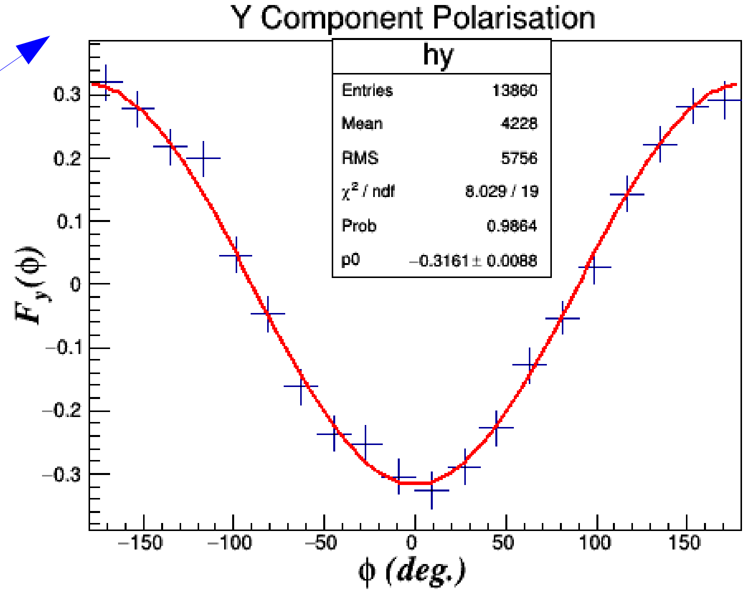

Spin Precession in 48D48 Dipole

48D48 TOSCA Field Map
Bare dipole

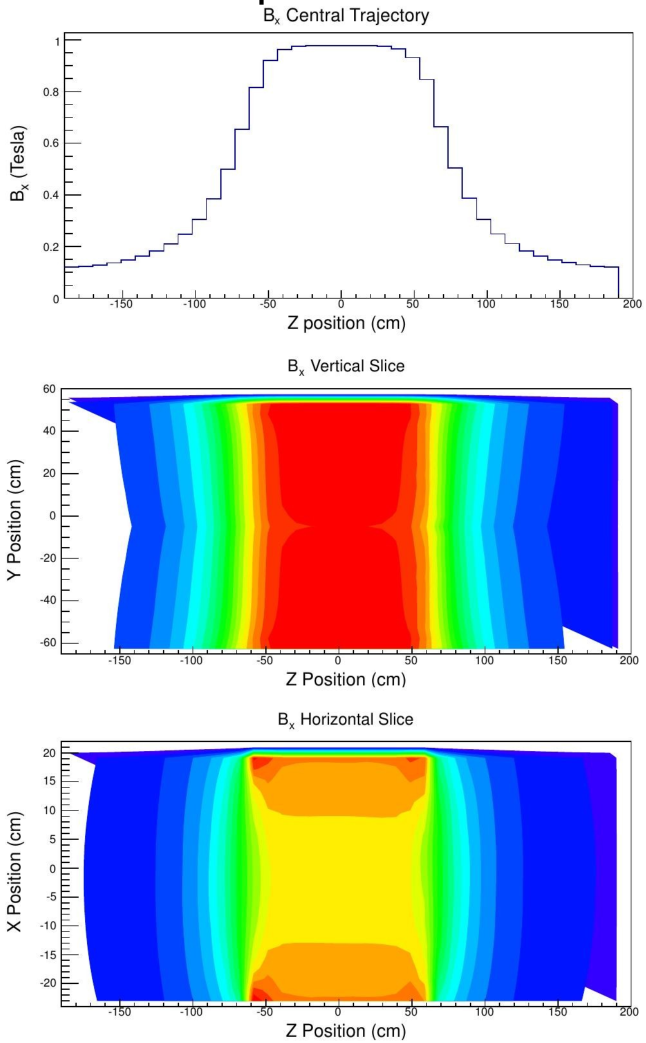

Analyser position dependence induced P_x

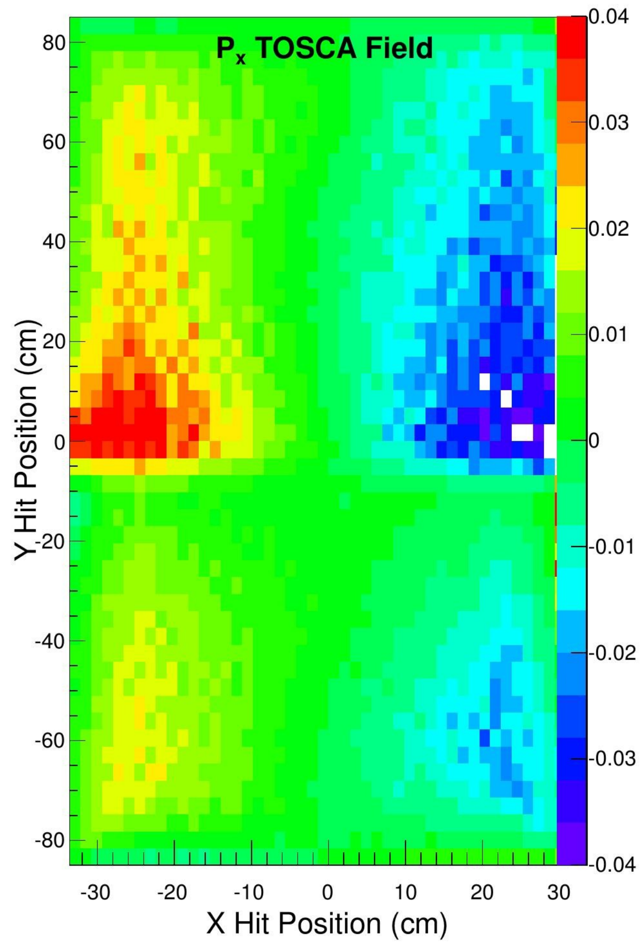

- Nucleon spin precession calculated in Geant-4
- TOSCA field map, no field clamps fitted
- Start 3 GeV/c neutron with spin (0,0,1) at target, track through dipole field, record spin components at analyser
- Max spin transfer z→ x ~4%
- Smoothly varying, can be corrected, analyser has good position resolution
- Max sys. error to P_x/P_z ~ 2.5%
- New calculation with updated TOSCA field necessary. New G4 also needs to be checked.

Precision @ L = 1.26×10^{38} cm^{-2}s^{-1}

$$\delta P = \sqrt{\frac{2}{N_{inc}\mathcal{F}^2}} \qquad R = \mu_n G_E^n / G_M^n$$

E_{beam} (GeV)	Q^2 (GeV/c)^2	p_n (GeV/c)	Rate (Hz)	FoM $\times 10^{-4}$	Time (hr)	δP	δR
2.2	2	1.72	1109	17.1	24	0.0035	0.008
4.4	4	2.89	122	4.4	48	0.014	0.044
6.6	6	3.97	29	1.9	150	0.026	0.10
8.8	9.3	5.82	3.2	0.9	750	0.051	0.22

- Estimates from ROOT-based and Geant-4 Monte Carlo models
- Geant-4 calculation in progress
  Detection efficiency ~ factor 2 higher than with ROOT model
  Effective A_y for ~ 25 g/cm^2 CH around 0.5 that of elastic n-p scattering, consistent with p-p scattering measurement (analyser thickness ~50 g/cm^2).
- R based on Glaster G_{En} and Kelly G_{Mn} EMFF parametrisation
- Expect overall systematic error to be ~3.0%

Comparison with E12-09-016

- E12-09-016 also uses BigBite and HCAL but has the polarised ^{3}He target (P ~ 60%)
- ^{2}H target offers a cleaner QE signal which results in lower systematic uncertainties

  Can we do better using recoil polarimetry?
- Increase luminosity ? Detector rates limitation Keep Pb shield to minimum
- Increase analyser thickness ? …rates, timing, multiple scattering
- Hydrogen analyser ? Could work with charge-exchange scattering...track exiting forward proton
- CH_2 analyser ? (as opposed to CH)...would require transparent polyethylene to detect Chernkov light.

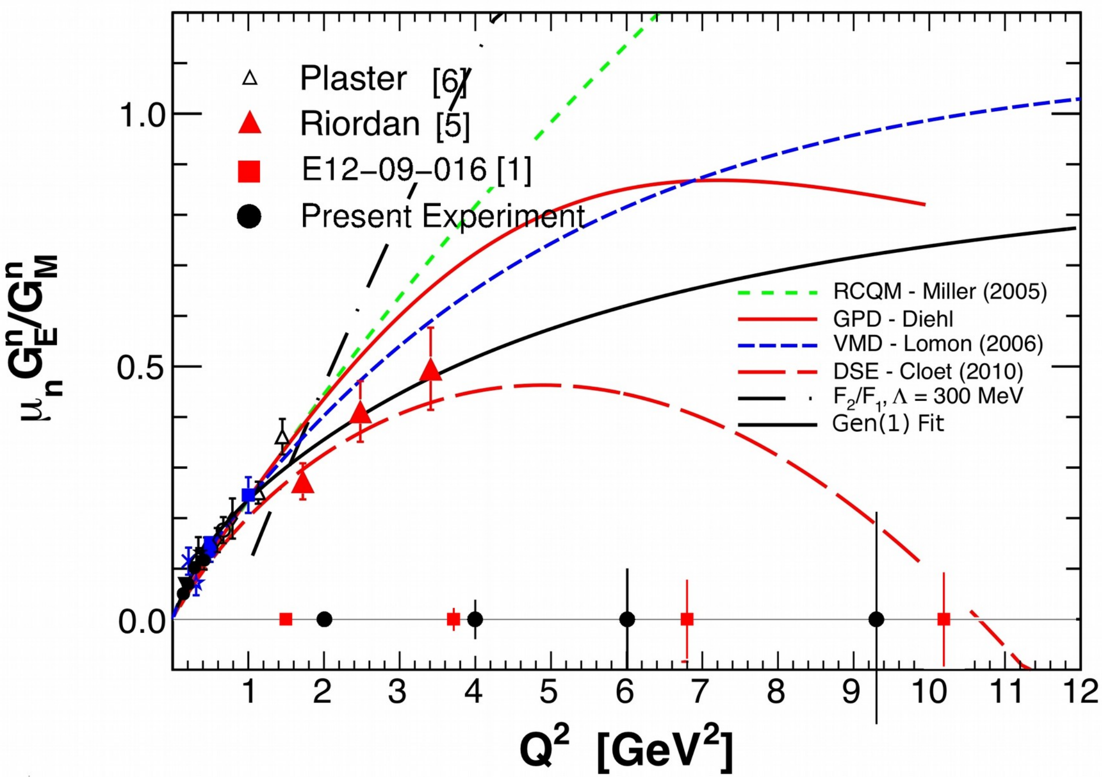

Hopefully predicted A_y values can be tested against new neutron measurements at Dubna p_n up to 4.5 GeV/c

New JLab proposal scheduled for 2017

Summary and Outlook

- BigBite and SBS configured as a polarimeter are highly suited to a double polarised, recoil-nucleon polarimetry measurement of G_{En}/G_{Mn}

  High precision low-to-medium Q^2 measurements will be possible with a relatively short measuring time.
- Reach to higher Q^2 is less certain due to uncertainty in the effective analysing power of the polarimeter at higher incident neutron momenta.
- **Polarised neutron A_y measurement proposed at JINR Dubna up to p_n = 4.5 GeV/c**, equivalent to $Q^2 \sim 7$ $(\mathrm{GeV/c})^2$. Test combination of analyser bars and calorimeter modules. Possibly run in 2016.

  Prototype 4x8 array of 4x4x250mm analyser bars constructed Glasgow

  This will also be available for Hall-A rates testing
- Charge-exchange scattering starts to dominate polarimeter FoM at p_n > 4.5 GeV/c

  This may allow for extension of recoil polarimetry technique to higher Q^2

  The Dubna experiment will distinguish forward-scattered neutrons from forward recoiling protons
- Monte Carlo simulations of the experiment continue in Geant-4 framework
- New JLab experimental proposal to 2017 PAC.

Thanks for your attention

Backup

Why a 2nd G_{En}/G_{Mn} Measurement

- **EMFF** fertile testing ground for models of nucleon structure
  QCD-related formalisms which calculate in the non-perturbative regime
  Dyson Swinger Equations, Lattice
  Does G_{Ep}/G_{Mp} continue to fall....zero crossing?
  Does G_{En}/G_{Mn} bend back and cross zero at high Q^2?
- With all 4 Sachs FF a flavour decomposition is possible (assuming negligible strange component of nucleon wave function).
  Q^2 range limited by G_{En} ...currently up to 3.5 GeV^2
  What do differences in u,d distributions show?
- EMFF are moments of GPDs. Absolutely necessary to have precise FF when extracting GPD from e.g. DVCS
- In terms of Q^2 range and precision, neutron measurements still lag way behind proton measurements
- Neutron measurements challenging...independent verification of results necessary
- QE signal much cleaner with ^2H target compared to ^3He
- ^2H experiment should, as far as possible, match range and precision of ^3He experiment. Up to now no recoil polarimetry measurement at $Q^2 > 1.5\ (GeV/c)^2$

University of Glasgow

Flavour Separation and Diquark Configurations

J.Segovia et al., *Understanding the Nucleon as a Borromean Bound State,* arXiv:1506.05112v1, 2015

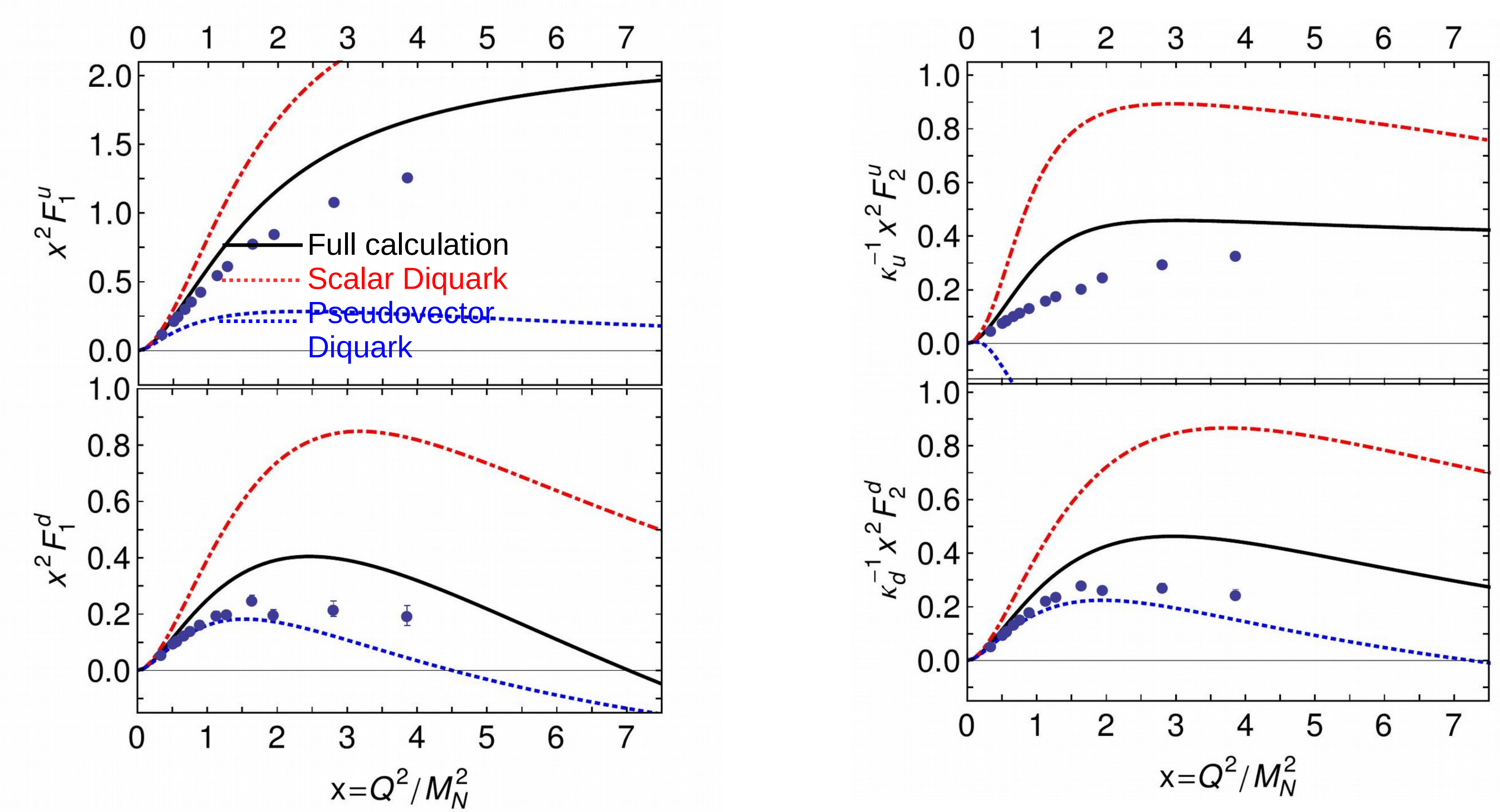

- Zero crossing location (if it exists) in F_1^d: relative probability of scaler and pseudo-vector diquarks in proton
- F_2^u more sensitive than F_1^u to interference between scalar and pseudo-vector diquark correlations
- Q^2 range of decomposition set by availability of G_{En} data. Verification of zero crossing in F_1^d, F_2^d requires extension of Q^2 range of G_{En}